**Contract No.:**

This manuscript has been authored by Savannah River Nuclear Solutions (SRNS), LLC under Contract No. DE-AC09-08SR22470 with the U.S. Department of Energy (DOE) Office of Environmental Management (EM).

**Disclaimer:**

The United States Government retains and the publisher, by accepting this article for publication, acknowledges that the United States Government retains a non-exclusive, paid-up, irrevocable, worldwide license to publish or reproduce the published form of this work, or allow others to do so, for United States Government purposes.

**Characterization of Undissolved Solids from the Dissolution of North Anna Reactor Fuel**

T. S. Rudisill, L. C. Olson, and D. P. DiPrete
Savannah River National Laboratory, Aiken, SC, USA

For all correspondence, contact Tracy S. Rudisill

Tracy S. Rudisill
Savannah River National Laboratory
Building 773-A
Aiken, SC 29808
email: tracy.rudisill@srnl.doe.gov
telephone: 803-725-2539
fax number: 803-725-2756

Key Words
Used nuclear fuel dissolution
Undissolved solids characterization
Tritium removal process

Running Title
Characterization of Undissolved Solids

# Characterization of Undissolved Solids from the Dissolution of North Anna Reactor Fuel


## ABSTRACT

Samples of undissolved solids (UDS) from the dissolution of North Anna reactor fuel were characterized to investigate the effects of using air or oxygen as the oxidant during tritium removal. The UDS composition data also supports the development of a waste form for disposal. There was no discernable effect of the oxidant used during the tritium removal process or the size fraction on the UDS composition. Scanning Electron Microscopy and energy dispersive (x-ray) spectroscopy was used to estimate the oxygen content of the UDS and was found potentially significant, on the order of 30% by mass and 80% by atom.


## INTRODUCTION

The US Department of Energy's Office of Nuclear Energy (DOE-NE) is responsible for the research, development, and demonstration activities that will ensure nuclear energy remains a viable option to meet future energy demands. One specific objective of DOE-NE's research and development roadmap is the development of sustainable nuclear fuel cycles which improve U resource utilization, maximize energy generation, minimize waste generation, improve safety, and complement institutional measures limiting proliferation risks.[1] Research and Development activities which support this objective include a coupled end-to-end (CETE) demonstration of used fuel reprocessing technology sponsored by DOE-NE's Fuel Cycle Technologies program at the Oak Ridge National Laboratory (ORNL).

Light water reactor (LWR) fuels were prepared for dissolution using a tritium removal step in the initial processing phase. The tritium removal process is a dry head-end method for removing tritium and other volatile fission products (e.g., $^{129}I_2$, $^{85}Kr$, Xe, and $^{14}C$ (as $^{14}CO_2$)) from used reactor fuel prior to aqueous processing. The tritium removal process is also an effective method to remove the fuel pellets from the cladding. The $UO_2$ reacts with $O_2$ to form $U_3O_8$ (equation 1) which results in volume expansion and a restructuring of the crystallite accompanied by particle crumbling.[2]

$$3UO_2 + O_2 \rightarrow U_3O_8 \quad (1)$$

Oxidation of LWR fuels prior to dissolution will increase the mass of residues which are insoluble in $HNO_3$ by as much as two or three times the amount generated by unoxidized fuel.[2] The amount of undissolved solids (UDS) from the dissolution of LWR fuels also generally increases with the burnup of the fuel.[2-3]

### Background

Used fuel from several reactors representing variations in fuel burnup and cooling times (time since discharge from reactor) were used in the CETE demonstration. Undissolved solids from the dissolution of two batches of North Anna reactor fuel were collected for characterization during Run No. 2 of the demonstration. Characteristics of the fuel are summarized in Table 1.

The two batches of North Anna fuel were treated for tritium removal at 600 °C using two different oxidation gases (air and oxygen).[4] The treated fuel was subsequently dissolved in 8 M $HNO_3$. The powdered fuel was slowly added to the dissolving solution over a 30-60 min period. The solution temperature was raised to 90 °C and held for 8 h during the dissolution. The UDS were recovered from the dissolving solution using a three stage filter assembly. The assembly was designed to utilize 185 mm Whatman® (ashless) filter paper with progressively

smaller pore sizes for solids recovery. The three UDS size fractions, grouped based on filter pore sizes and obtained from the fuel, were > 20-25 μm, > 8 μm, and > 2.7 μm. Smaller particles may have been filtered out by the filter cake products in any or all stages but were not collected intentionally.

The three different size fractions from each dissolution were subsequently dried and collected in individual containers. A summary of the UDS samples collected from the North Anna fuel is provided in Table 2.

### Objectives

An understanding of the effect of the tritium removal process on the composition of the UDS is desired to quantify the amount of fissionable materials which were not solubilized during the CETE dissolutions. The composition of the solids is also needed for the development of a waste form for the disposal of the UDS from an industrial scale plant. To address these needs, the six UDS samples from the North Anna reactor fuel were shipped to the Savannah River National Laboratory (SRNL) for characterization. Characterization activities initially included the dissolution of multiple samples of the UDS for subsequent radiochemical and elemental analyses. Samples of the solids were also examined by scanning electron microscopy (SEM) and X-ray diffraction (XRD). Some of the characterization and analysis can be found separately in previous SRNL reports [5-6], but are compiled herein with more in-depth analysis and discussion. The experimental methods used to prepare and analyze the samples and a discussion of the analytical results are provided in the following sections.

## EXPERIMENTAL

The six samples of UDS generated from the North Anna reactor fuel (Table 2) during CETE Run No. 2 were shipped to SRNL. When the UDS were packaged at ORNL, the dried solids on each filter paper were placed in a glass sample bottle which was then placed inside a screw-top stainless steel container. Three samples were selected from the six samples received from ORNL for characterization. The selection provided comparisons between the tritium removal conditions (i.e., oxidation gas) and the size fractions of the collected solids. The selected samples were NADS-1, Stage 1 and Stage 3 and NADS-2, Stage 3.

### UDS Dissolution

Due to the high radiation doses associated with the UDS, the samples were placed in an intermediate level hot cell to prepare the three samples for dissolution. The solids were black in appearance and were relatively free flowing. To prepare the UDS for dissolution, nominally 0.25 g of the selected samples were transferred to small stainless steel vials. When the solids were removed from the NADS-1, Stage 3 and NADS-2, Stage 3 samples, it was apparent that small pieces of filter paper were intimately mixed with the solids. Separation of the UDS from the filter paper was not practical. The vials were subsequently transferred to the SRNL Shielded Cells for dissolution.

The three UDS samples were prepared for dissolution by fusing the solids with a mixture of $Na_2O_2$ and NaOH. A blank which only contained the reagents required to perform the fusion was also prepared for dissolution. To perform a fusion, an approximate 0.25-g solids sample was transferred to a weighed, etched, 55-mL Zr metal crucible. The two samples which contained small pieces of filter paper were heated at 675 °C for 10 min to ash the paper; the crucible was subsequently reweighed. A fusion was performed by adding 1.5 g of $Na_2O_2$ and 1.0 g of NaOH

to a crucible and heating at 675 °C for 10 min. A Zr metal lid was placed on the crucible during heating. After cooling for 3 or 4 min, approximately 5 mL of deionized water were slowly added to a crucible to begin to dissolve some of the salts. The liquid and a portion of the solids were then transferred to a 250 mL volumetric flask. The crucible was rinsed with several 15- to 20-mL aliquots of deionized water. After adding, the water was swirled in the crucible and transferred to the volumetric flask. The crucible was rinsed until no solids remained. A 25-mL aliquot of concentrated $HNO_3$ was then added to the crucible. The crucible was swirled and the $HNO_3$ was transferred to the volumetric flask. To complete the transfer, a final 10-mL aliquot of deionized water was added to the crucible, swirled, and transferred to the volumetric flask. The volumetric flask (now containing approximately 200 mL of liquid) was capped and shaken to dissolve the remainder of the fused solids. A 1-mL aliquot of 30 vol % $H_2O_2$ was added to the volumetric flask prior to dilution to volume with deionized water to ensure complete oxidation of metals. All of the fused solids dissolved resulting in dark grey to black solutions.

**Solution Analysis**

Aliquots of solutions containing the dissolved UDS and the blank were removed from the SRNL Shielded Cells for radiochemical and elemental analyses. The analyses performed included: liquid scintillation counting (for total alpha and beta emitters), gamma pulse height analysis (GPHA) (for total gamma emitters), 2-thenoyltrifluoroacetone extraction (TTA) /alpha pulse height analysis (APHA) (for $^{238}$Pu and $^{239-240}$Pu), Am/Cm/Cf isotopes, $^{90}$Sr, $^{99}$Tc, inductively-coupled plasma mass spectrometry (ICP-MS) (for fission products, actinides, and U/Pu isotopics), and inductively-coupled plasma atomic emission spectroscopy (ICP-AES) (for low molecular weight fission and corrosion products). A brief description of each analysis method is provided below.

- Liquid Scintillation Counting – Aliquots of sample were added to the liquid scintillation cocktail and analyzed for gross alpha and gross beta activity using liquid scintillation analysis. Alpha/beta spillover was determined for each aliquot analyzed, and subsequently used for accurately determining alpha and beta activity by the addition of a known amount of Pu to an identical aliquot of each sample.
- GPHA – Aliquots of sample were analyzed by coaxial high purity germanium gamma-ray spectrophotometers to measure the gamma-emitting radionuclides present.
- TTA Extraction/APHA – Aliquots of samples were initially spiked with a $^{236}$Pu tracer. The Pu was extracted from the matrix using TTA following a series of oxidation-state adjustments. The TTA extracts were mounted on stainless steel counting plates and counted for $^{238}$Pu and $^{239-240}$Pu using passivated, implanted, planar silicon (PIPS) alpha spectrometers. The separation efficiency was based on the $^{236}$Pu recovery.
- Am/Cm/Cf Isotopes – The Am, Cm and Cf isotopes were extracted from the sample matrix using a CMPO/TBP-based solid phase extractant and purified further with an HDEHP-based solid phase extractant. The $^{241, 242m, 243}$Am, $^{243, 245, 247}$Cm, and $^{249, 251}$Cf concentrations were measured using low energy photon/X-ray, thin-windowed, semi-planar high purity germanium spectrometers. The $^{242, 244}$Cm concentrations were measured using PIPS alpha spectrometers. An $^{243}$Am tracer is normally used to correct the analytical results for any losses during the radiochemical separations; however, the presence of $^{243}$Am in the samples precluded its addition. The efficiency of the separations was determined from the $^{154}$Eu measured by GPHA.

- $^{90}Sr$ – Aliquots of sample were initially spiked with natural Sr carrier. The Sr isotopes were extracted from the matrix using a crown ether-based solid phase extractant. The $^{90}Sr$ concentrations were measured by liquid scintillation counting. Elemental Sr carrier yields were measured for each aliquot by neutron activation analysis and were used to correct the $^{90}Sr$ value for any Sr losses incurred during the radiochemical separations.
- $^{99}Tc$ – A $^{99m}Tc$ tracer was generated in the SRNL $^{252}Cf$ neutron activation analysis facility by activating $^{99}Mo$ to produce $^{99m}Tc$ by neutron irradiation. The $^{99m}Tc$ was extracted from the $^{99}Mo$ target material with methyl isobutyl ketone. The $^{99m}Tc$ tracer was added to aliquots of the samples. The Tc species were extracted from the sample using a solid extractant based on Aliquat-336™. The $^{99}Tc$ concentrations were measured by liquid scintillation counting. The $^{99m}Tc$ yields were measured for each aliquot with a NaI well gamma spectrometer and were used to correct the $^{99}Tc$ values for any Tc losses incurred during the radiochemical separations.
- ICP-MS – An elemental analysis for mass to charge (m/z) values greater than 88 was performed by ICP-MS.
- ICP-AES – An elemental analysis for selected (lower molecular mass) analytes was performed by ICP-AES.

**Physical Characterization**

Solids from sample NADS-1, Stage 1 were examined by XRD. The solids from samples NADS-1, Stage 3 and NADS-2, Stage 3 were not examined by XRD due to the time and resulting exposure required to remove the filter paper fragments from the UDS. A small portion of the UDS from samples NADS-1, Stage 1 and Stage 3 and NADS-2, Stage 3 were also examined by SEM/energy dispersive (x-ray) spectroscopy (EDS). The NADS-1, Stage 1 sample was subsequently analyzed in more depth than the others, and semi-quantitative EDS data compared to the ICP-MS and ICP-AES results. The ashing step was not necessary for SEM/EDS analysis. Photomicrographs of the solids and wide-area raster scans were obtained for each sample. The raster scans provide qualitative information concerning the composition of the solids which were examined. Although imperfect, the EDS semi-quantitative analysis can give an indication of the oxide levels present in the UDS following the tritium pretreatment and dissolution processes.

## RESULTS AND DISCUSSION

### Solution Analysis

The measured concentrations from the radiochemical and elemental analyses for the UDS samples are provided in the following sections. A discussion of the results is provided for each analytical method including any issues associated with the analysis.

*Liquid Scintillation Counting*

The total alpha and nonvolatile beta emitters for each UDS sample are given in Table 3. The high beta activity of the UDS samples, primarily from $^{90}Sr$, $^{106}Ru$, $^{125}Sb$, and $^{154}Eu$, interfered with the alpha counting. Due to the interferences, the values given for the alpha emitters in the UDS samples are upper limits.

*Gamma Pulse Height Analysis*

The concentrations of the primary gamma emitters for each UDS sample are given in Table 4.

*Pu TTA Extraction/Alpha Pulse Height Analysis*

Since the analytical method measures a combined activity for $^{239}$Pu and $^{240}$Pu, the relative ratio of the activities of the isotopes is required to calculate the Pu isotopic concentrations. To perform this calculation, the data from the ICP-MS analysis were used to calculate the relative weight and activity percentages of the two isotopes. The Pu isotopic concentrations are shown in Table 5. The Pu isotopic concentrations in each UDS sample were subsequently used to calculate the Pu isotopics. The results of the calculations are shown in Table 6.

*Am/Cm/Cf Isotopes*

The concentrations of the Am, Cm, and Cf isotopes for each UDS sample are given in Table 7.

*$^{90}$Sr*

The $^{90}$Sr concentration in each of the UDS samples is given in Table 8.

*$^{99}$Tc*

The $^{99}$Tc concentration in each of the UDS samples is given in Table 8.

*Inductively-Coupled Plasma Mass Spectrometry*

In general, the cell blank contained very little mass with the exception of stable Zr isotopes (i.e., $^{90}$Zr, $^{91}$Zr, $^{92}$Zr, $^{94}$Zr, and $^{96}$Zr). The Zr present in the blank was from the use of a Zr metal crucible to perform the $Na_2O_2$/NaOH fusions. Therefore, the stable Zr concentrations measured in the blank were used to correct the stable Zr isotopic concentrations measured in the UDS samples since the fusions were also performed using the same crucibles. To correct the concentrations, the stable Zr concentrations measured in the blank were subtracted from the concentrations measured in each sample. The corrected values are included in Table 9. The corrections assume that the Zr contamination from the crucibles used to fuse the UDS samples was the same as the Zr contamination from the crucible used to prepare the blank. The relative standard deviation (RSD) for the isotopic concentrations given in the table was calculated from two scans and is a measure of the analytical precision. The accuracy of the measured concentrations is within ± 20%.

The majority of the mass measured by the ICP-MS analyses ranged between m/z values of 90 and 108 and from 238 to 240. These isotopes included the transition metal fission products Zr, Mo, Ru, Tc, Pd, and Ag, $^{238}$U, and $^{239\text{-}240}$Pu. The material balance closure for the ICP-MS analysis was poor. The analyses only account for 40 to 50% of the material dissolved based on the isotopic concentrations. If an assumption is made that the isotopes were present as oxides, the material balance closures improved to 55 to 65%. The instrument used to perform the ICP-MS analyses could only quantify isotopes with an m/z value greater than 88 due to spectral interferences at the lower values. There were undoubtedly elements with atomic masses less than 88 present in the UDS samples; although, a majority of these elements were probably not generated by fission in the North Anna fuel. The fission yields below an atomic mass of 88 are very low.[7] It is likely that a portion of the remaining UDS mass accumulated during the tritium pretreatment and dissolution processes. Elements such as Fe, Cr, and Ni from the corrosion of stainless steel processing equipment and Si from process water and other sources

would have accumulated in the UDS. The contribution to the material balance closure of these and other elements which were not quantified by the ICP-MS analyses is discussed in the following section.

The ICP-MS analysis also provides information about the U isotopics in the used North Anna reactor fuel. The concentrations of $^{235}U$, $^{236}U$, and $^{238}U$ given in Table 9 were used to calculate the weight percentages of these isotopes. The isotopic information is given in Table 6.

*Inductively-Coupled Atomic Emission Spectrometry*

The elemental concentrations obtained from the ICP-AES analysis for the UDS samples are shown in Table 10. In general, the cell blank contained very little mass with the exception of Zr. The Zr present in the blank was from the use of the Zr metal crucible to perform the $Na_2O_2$/NaOH fusions. Therefore, the stable Zr concentrations measured in the blank were used to correct the stable Zr isotopic concentrations measured in the UDS samples in the same manner as performed for the ICP-MS analyses. Small corrections were also made for Ag, Al, Ca, Fe, and Sr. The corrected values are included in Table 10. The relative standard deviations (RSD) for the isotopic concentrations given in the table were calculated from two scans and are a measure of the analytical precision. The accuracy of the measured concentrations is generally within ± 20%. The RSD for the stable Zr isotopes were calculated using standard propagation of error techniques.

The ICP-AES analyses quantify a number of elements with m/z values less than 88; concentrations for elements of interest such as Fe, Cr, Ni, and Si are provided. If the assumption is made that the elements not quantified by the ICP-MS analyses were present as oxides, the material balance closures improve by approximately 5% to 60 to 70%. The uncertainty of the analyses due to the relatively small sample sizes and trace level concentrations of many elements could likely account for the missing mass.

**Physical Characterization**

*X-ray Diffraction*

Solids from sample NADS-1, Stage 1 were examined by XRD. Two solid phases were identified by the analysis. Ruthenium oxide was identified; although, the Ru was probably present as a mixed oxide containing Pd. The second phase identified was a zirconium tungsten oxide hydroxide hydrate which probably contained Mo instead of W. The two compounds are isostructural.

*Scanning Electron Microscopy*

A small portion of the three UDS samples was examined by SEM. After the initial examination, a more in-depth semi-quantitative examination was undertaken using the NADS-1, Stage 1 sample.

Initial Characterization

Solids taken from UDS samples NADS-1, Stage 1 and Stage 3 and NADS-2, Stage 3 were all examined by SEM. A photomicrograph of the solids from the NADS-1, Stage 1 sample is shown as an example in Figure 1. The solids from the Stage 1 sample had the appearance of an agglomerated filter cake as a result of the collection process in the filtration assembly. In the filter cake, after larger particles were screened out, the filtered material itself acted as a filter to further remove finer particles, and formed a conglomeration which when dried had a ‘cracked

mud-like' appearance. The solids in the photomicrographs of the Stage 3 samples were much more dispersed since the amount of solids collected was significantly less than the amount of solids collected in the Stage 1 sample. The solids were also intimately mixed with small pieces of filter paper.

A wide-area raster scan is also provided with the photomicrograph of the Stage 1 sample (Figure 1). The raster scan provides qualitative information concerning the composition of the solids. The raster scans for the solids from all three samples were very similar. The presence of Al, Fe, Mo, Pd, Ru, S, Si, U, and Zr were identified in the solids from all three samples. Other elements observed in the scans included Ca, Cu, Cr, and Ta.

Semi-Quantitative EDS Characterization

A second SEM/EDS analysis of NADS-1, Stage 1, prepared two samples on separate SEM stages. First, conductive carbon tape was applied to the top of the stages for a semi-quantitative analysis of the EDS data. For the first sample, the stage was then pushed directly into the UDS container, with some large particles sticking to the conductive tape. For the second sample, some UDS particles were portioned into a new/un-used unglazed terracotta mortar, and ground using a new/un-used matching unglazed terracotta pestle; another SEM stage with conductive tape was then pushed into the resultant crushed powder. Prior to SEM/EDS, because the samples were potentially non-conductive, the SEM stages with samples were coated with carbon using a model 12560 EFFA Mark II carbon coater.

Figure 2 shows an SEM image of the UDS filter cake material. The corresponding EDS semi-quantitative analysis for the uncrushed UDS particle (Table 11) shows that the UDS is, in general, high in oxide content. For the semi-quantitative analysis, the focus at the time was on determining and confirming the composition of the UDS, so bulk elements that were known to not be present (such as Fe, Ni, Al, Si, K, Cr, etc.) or below reasonable EDS detection limits for semi-quantitative analysis, were screened out of the element analysis results. Caution is advised when interpreting EDS semi-quantitative analysis, and inaccuracies of several percent can be expected from actual values. However, qualitative judgements can still often be made.

To lessen the impact of possible surface effects on the incident electron beam that would skew results from the uncrushed filter cake UDS sample, SEM/EDS was also performed on multiple crushed UDS samples, (Figure 3 and Table 11).

Due to the conglomerative nature of the UDS, higher magnification for more precise knowledge of the electron beam incidence was needed, and was performed for the crushed samples (Figure 4 and Table 11). Results in mass percent are included in Table 11 for later analysis.

EDS x-ray maps (Figure 5) show that the light particles in Figure 4 are enriched in elements known to be present in epsilon phase particles, namely: Mo, Ru, Tc, Rh, Pd, and Te.[8] Epsilon phase particles are very stable particles that form in used nuclear fuel during reactor operation.

**Comparison of Semi-Quantitative EDS Characterization to ICP-MS and ICP-AES Analyses**

The ICP-MS and ICP-AES results from NADS-1, Stage-1 are discussed here as they pertain to the samples analyzed by SEM/EDS. There are several simplifications to the ICP-MS and ICP-AES data presented here: 1) because the UDS fusion step occurred in Zr metal crucibles, the Zr signal in all ICP-MS and ICP-AES techniques is suspect, and caution is urged in its

interpretation due to the Zr signal from the sample blank, 2) the mass percent output is given in atomic mass units (amu) for the ICP-MS results, so when several isotopes share atomic masses, there can be some ambiguity as to the actual elemental distribution; for this analysis, it is assumed that ambiguous results are split evenly among the possible likely elements, 3) where possible, ICP-AES was used to check the second caveat, and 4) the lower detection limit for the ICP-MS employed at SRNL was ~88 amu, and neither ICP-MS or ICP-AES was able to give a metric for the oxide content. The results with the aforementioned assumptions are presented in Table 12, with elements that were deemed too small in concentration to be listed on their own combined in a category called 'other'; the large unknown concentration was back calculated using conservation of mass principles.

The aqueous chemical analysis had presented ambiguous Zr levels due to Zr contamination from the crucibles used in the UDS dissolution process, and also resulted in a high unknown component believed to be oxygen. While XRD appeared to back-up the oxygen hypothesis, SEM/EDS data provides a better metric of the oxide content. It was found that the UDS sample analyzed by EDS was very high in oxygen on average, accounting for ~80% of the atomic fraction and ~30% of the mass fraction of the EDS points analyzed. Because the EDS analysis analyzed just specific points on the surface, the majority of the aqueous chemical analysis should be used for getting a global understanding of the chemical make-up of the samples, but the EDS point analyses support the hypothesis that the large unknown components in the ICP-MS results were primarily oxygen.

Special effort was made to find points that could be identified as unoxidized metal, but as the results show, none were conclusively found. However, there is some evidence that the lightest regions in Figure 4 may be epsilon particles; whether they are oxidized cannot be determined conclusively. Although, evidence appears to indicate a high level of oxidation, it is also possible the surrounding matrix is contributing to the EDS x-ray signal due to the small particle size. According to Cui et al. [8], epsilon particles tend to have the composition on average shown in Table 13, and are on the order of microns in size (consistent with the particles observed in Figure 4), with the largest fraction being 0.5 to 1.0 μm. Tellurium has been found by some researchers, but not always.[8]

Comparing the EDS point analysis data from the proposed epsilon particles shown in Figure 4 and in Table 13, mass ratios of Mo (chosen arbitrarily over the other epsilon elements) show some similarity between the analyses and proposed values from literature (Table 14). While the ratios with Tc, Rh, and Te, appear to diverge, it should be noted that the statistical significance of those specific ratios is likely low due to the low concentrations of the elements.

## CONCLUSIONS

Three samples of UDS generated from the dissolution of North Anna reactor fuel at ORNL were characterized to investigate the effect of air and oxygen as the oxidant during tritium removal on the solids composition. The measured UDS composition also supports the potential development of a metal waste form or other advanced waste forms for disposal of the solids from an industrial scale facility. The characterization activities included solids dissolution followed by radiochemical and elemental analyses. Samples of the UDS were also examined by SEM and XRD. Following the analyses, we concluded there was no discernable effect of the oxidant used during the tritium removal process or the size fraction of the collected material on the UDS composition.

We found that the UDS samples contained high beta activity. The principle beta-emitting isotopes were $^{90}Sr$, $^{106}Ru$, $^{125}Sb$, and $^{154}Eu$. The high contact dose from the beta activity was the principle handling issue. The primary alpha activity in the UDS was from $^{238}Pu$ and $^{244}Cm$. The total Pu in the UDS samples ranged between 1500 and 6000 μg/g. The results from the ICP-MS analysis showed that the UDS samples contained mostly transition metal fission products, $^{238}U$, and $^{239\text{-}240}Pu$. The most abundant metals identified were Zr, Mo, Tc, Ru, Rh, Pd, Ag, Cd, U, and Nb based on the combined ICP-MS and ICP-AES analyses. The ICP-MS and ICP-AES analyses could only accounted for 60 to 70% of the mass of material dissolved on an oxide basis. The uncertainty of the analyses introduced during the remote preparation of the relatively small UDS samples as well as the uncertainty associated with the analytical methods could likely account for much of the missing mass. SEM and EDS analysis was used to indicate the oxygen content of the undissolved NADS-1, Stage 1 solids and was found to potentially be significant, on the order of 30% by mass and 80% by atom. Furthermore, evidence was found of epsilon particles surrounded in a $ZrO_2$ matrix.

## ACKNOWLEDGEMENTS

The work was supported by the US Department of Energy's Office of Nuclear Energy. The Savannah River National Laboratory is operated by Savannah River Nuclear Solutions under contract number DE-AC09-08SR22470.

## REFERENCES

1. *Nuclear Energy Research and Development Roadmap – Report to Congress*, (2010) United States Department of Energy Office of Nuclear Energy, Washington, DC.
2. Lewis, B. E. (1982) *A Review of Solid/Liquid Separation Methods and Procedures for Fuel Reprocessing*, ORNL/TM-7968, Oak Ridge National Laboratory, Oak Ridge, TN.
3. Lausch, J., Berg, R., Koch, L., Coquerelle, M., Glatz, J.-P., Walker, C. T., and Mayer, K (1994) *Dissolution Residues of Highly Burnt Nuclear Fuels*, J. Nucl. Mater., 208: 73-80.
4. Spencer, B. B., DelCul, G. D., Jubin, R. T., Bailey, P. D., Owens, R. S., Ramey, D. W., and Collins, E. D. (2009) *Voloxidation Processing of CETE Run 2 Fuels: Experimental Results*, ORNL/TM-2009/nnn (draft), Oak Ridge National Laboratory, Oak Ridge, TN.
5. Rudisill, T. S., Emory, S. J., Click, D. R., and DiPrete, D. P. (2011) *Characterization of Undissolved Solids from the Dissolution of North Anna Reactor Fuel*, FCRD-SEPA-2011-000024 and SRNL-STI-2010-00807, Savannah River National Laboratory, Aiken, SC.
6. Olson, L. C. (2011) *FY2011 Status Report: Oxide Incorporation In Iron Based Alloy Waste Forms*, FCRD-SWF-2011-000222 and SRNL-STI-2011-00429, Savannah River National Laboratory, Aiken, SC.
7. Baum, E. M., Know, H. D., and Miller, T. R. (2002) *Chart of the Nuclides*, 16th ed – revised to 2002, Knolls Atomic Power Laboratory, Niskayuna, NY.
8. Cui, D., Low, J., Sjostedt, C., and Spahiu, K. (2004) *On Mo-Ru-Tc-Pd-Rh-Te alloy particles extracted from spent fuel and their leaching behavior under Ar and $H_2$ atmospheres*, Radiochim. Acta, 92: 551–555.

TABLE 1
North Anna used reactor fuel

| | |
|---|---|
| Initial $^{235}U$ enrichment | 4.199% |
| Cladding | M5® |
| Fuel burnup | 63-70 GWd/MTIHM |
| Cool Time | ~ 6 y (Discharge date May 1, 2004) |

TABLE 2
UDS collected from North Anna reactor fuel

| UDS Designation | Oxidation Gas | Size Fraction (μm) |
|---|---|---|
| NADS-1, Stage 1 | Air | > 20-25 |
| NADS-1, Stage 2 | Air | > 8 |
| NADS-1, Stage 3 | Air | > 2.7 |
| NADS-2, Stage 1 | Oxygen | > 20-25 |
| NADS-2, Stage 2 | Oxygen | > 8 |
| NADS-2, Stage 3 | Oxygen | > 2.7 |

TABLE 3
Total alpha and beta emitters in UDS samples

| Sample ID | alpha count (MBq/g) | 1 sigma uncertainty (%) | nonvolatile beta count (MBq/g) | 1 sigma uncertainty (%) |
|---|---|---|---|---|
| Cell Blank | <1.31 | MDL | <1.03 | MDL |
| NADS-1 Stg 1 | <1010 | upper limit | 13700 | 10 |
| NADS-1 Stg 3 | <212 | upper limit | 5070 | 10 |
| NADS-2 Stg 3 | <657 | upper limit | 13200 | 10 |

MDL – method detection limit

TABLE 4
Primary gamma emitters in UDS samples

| Isotope | Cell Blank (µg/g) | NADS-1 Stage 1 (µg/g) | 1 sigma uncertainty (%) | NADS-1 Stage 3 (µg/g) | 1 sigma uncertainty (%) | NADS-2 Stage 3 (µg/g) | 1 sigma uncertainty (%) |
|---|---|---|---|---|---|---|---|
| $^{60}$Co | MDA | 0.0478 | 5.9 | 0.0184 | 33.1 | 0.0363 | 12.3 |
| $^{106}$Ru | MDA | 59.0 | 5.0 | 15.8 | 5.0 | 50.8 | 5.0 |
| $^{110m}$Ag | MDA | ND | NA | ND | NA | 0.0581 | 5.0 |
| $^{125}$Sb | MDA | 37.2 | 5.0 | 12.0 | 5.0 | 31.0 | 5.0 |
| $^{134}$Cs | MDA | 1.66 | 5.0 | 4.49 | 5.0 | 4.25 | 5.0 |
| $^{137}$Cs | MDA | 84.5 | 5.0 | 229 | 5.0 | 215 | 5.0 |
| $^{154}$Eu | MDA | 0.727 | 16.6 | 1.37 | 10.9 | 2.17 | 5.0 |

MDA – minimum detection of analysis
ND – not detected
NA – not applicable

TABLE 5
Pu isotopic concentrations in UDS samples

| Sample ID | $^{238}$Pu (µg/g) | $^{239}$Pu (µg/g) | $^{240}$Pu (µg/g) | $^{238\text{-}240}$Pu (µg/g) |
|---|---|---|---|---|
| NADS-1 Stg 1 | 373 | 3374 | 1814 | 5561 |
| NADS-1 Stg 3 | 90 | 1071 | 453 | 1614 |
| NADS-2 Stg 3 | 352 | 3045 | 1825 | 5222 |

TABLE 6
Pu isotopics for UDS samples

| Sample ID | $^{238}$Pu (wt %) | $^{239}$Pu (wt %) | $^{240}$Pu (wt %) | $^{235}$U (wt %) | $^{236}$U (wt %) | $^{238}$U (wt %) |
|---|---|---|---|---|---|---|
| NADS-1 Stg 1 | 6.70 | 60.7 | 32.6 | 0.50 | 0.57 | 98.93 |
| NADS-1 Stg 3 | 5.59 | 66.3 | 28.1 | 0.43 | 0.76 | 98.81 |
| NADS-2 Stg 3 | 6.74 | 58.3 | 34.9 | 0.47 | 0.70 | 98.82 |

Table 7
Transplutonium analysis for UDS samples

| Isotope | Cell Blank (µg/g) | 1 sigma uncert. (%) | NADS-1 Stage 1 (µg/g) | 1 sigma uncert. (%) | NADS-1 Stage 3 (µg/g) | 1 sigma uncert. (%) | NADS-2 Stage 3 (µg/g) | 1 sigma uncert. (%) |
|---|---|---|---|---|---|---|---|---|
| $^{241}$Am | 0.0478 | 24.4% | 67.5 | 18.1% | 43.1 | 13.0% | 79.2 | 8.70% |
| $^{242m}$Am | <0.000266 | MDA | 0.194 | 18.7% | <0.147 | MDA | 0.144 | 55.9% |
| $^{243}$Am | <0.000178 | MDA | 15.3 | 18.1% | 26.1 | 19.5% | 42.1 | 8.70% |
| $^{242}$Cm | <0.000000974 | MDA | 0.000708 | 18.7% | <0.000538 | MDA | 0.000527 | 55.9% |
| $^{243}$Cm | <0.00626 | MDA | <0.0796 | MDA | 0.222 | MDA | <0.269 | upper limit |
| $^{244}$Cm | <0.00332 | upper limit | 18.2 | 18.1% | 27.1 | 23.0% | 63.3 | 28.7% |
| $^{245}$Cm | <1.51 | MDA | <19.6 | MDA | <54.6 | MDA | <17.0 | MDA |
| $^{247}$Cm | <4170 | MDA | <19700 | MDA | <53400 | MDA | <12600 | MDA |
| $^{249}$Cf | <0.105 | MDA | <0.463 | MDA | <1.30 | MDA | <0.285 | MDA |
| $^{251}$Cf | <0.205 | MDA | <0.952 | MDA | <2.64 | MDA | <0.634 | MDA |

MDA – minimum detection of analysis

TABLE 8
$^{90}$Sr and $^{99}$Tc concentrations in UDS samples

| Sample ID | $^{90}$Sr (µg/g) | 1 sigma uncertainty (%) | $^{99}$Tc (µg/g) | 1 sigma uncertainty (%) |
|---|---|---|---|---|
| Cell Blank | <0.0183 | MDA | <1.55 | MDA |
| NADS-1 Stg 1 | 19.7 | 5.83 | 17700 | 7.96 |
| NADS-1 Stg 3 | 45.6 | 6.01 | 5290 | 8.38 |
| NADS-2 Stg 3 | 55.7 | 5.98 | 13800 | 8.21 |

MDA – minimum detection of analysis

TABLE 9
Elemental concentration from ICP-MS analysis

| Isotope(s) | Cell Blank (μg/g) | RSD (%) | NADS-1 Stage 1 (μg/g) | RSD (%) | NADS-1 Stage 3 (μg/g) | RSD (%) | NADS-2 Stage 3 (μg/g) | RSD (%) |
|---|---|---|---|---|---|---|---|---|
| $^{88}$Sr | | | 45.9 | 46.4 | | | | |
| $^{89}$Y | 40.7 | 6.75 | 52.9 | 15.8 | | | 78.8 | 7.82 |
| $^{90}$Zr | 40300 | 3.14 | 18300 | 0.96 | 125000 | 1.90 | 30700 | 1.24 |
| $^{91}$Zr | 8590 | 0.32 | 7810 | 0.21 | 28540 | 0.39 | 12700 | 2.70 |
| $^{92}$Zr | 13800 | 0.20 | 10800 | 0.35 | 44900 | 0.31 | 17500 | 0.87 |
| $^{93}$Zr/$^{93}$Nb | 54.7 | 14.0 | 5430 | 5.43 | 2080 | 6.42 | 7810 | 0.90 |
| $^{94}$Zr | 14300 | 0.11 | 10400 | 0.33 | 47300 | 0.45 | 18200 | 2.95 |
| $^{95}$Mo | | | 17400 | 1.19 | 5260 | 3.64 | 21800 | 1.70 |
| $^{96}$Zr/$^{96}$Mo | 2410 | 4.16 | 9410 | 5.02 | 10300 | 1.20 | 13400 | 1.53 |
| $^{97}$Mo | | | 19700 | 0.92 | 5870 | 0.30 | 24100 | 0.10 |
| $^{98}$Mo | | | 20600 | 0.91 | 6080 | 2.44 | 25500 | 1.61 |
| $^{99}$Ru/$^{99}$Tc | | | 15600 | 0.13 | 4410 | 1.99 | 11500 | 3.36 |
| $^{100}$Ru/$^{100}$Mo | | | 31900 | 0.78 | 9590 | 1.19 | 36600 | 2.61 |
| $^{101}$Ru | | | 37600 | 1.34 | 11100 | 4.07 | 31700 | 2.30 |
| $^{102}$Ru | | | 43700 | 4.71 | 13200 | 2.25 | 38900 | 1.78 |
| $^{103}$Rh | 45.7 | 2.55 | 17000 | 2.05 | 5080 | 2.02 | 14200 | 9.26 |
| $^{104}$Ru/$^{104}$Pd | | | 47600 | 0.93 | 13600 | 1.84 | 40000 | 3.04 |
| $^{105}$Pd | | | 19900 | 0.55 | 4780 | 1.01 | 15700 | 2.96 |
| $^{106}$Pd/$^{106}$Cd | 363 | 1.62 | 22700 | 4.04 | 6850 | 2.22 | 18000 | 1.19 |
| $^{107}$Pd/$^{107}$Ag | 136 | 11.1 | 12900 | 1.87 | 3890 | 7.54 | 10400 | 2.06 |
| $^{108}$Pd/$^{108}$Cd | 132 | 2.37 | 8220 | 1.43 | 2510 | 3.37 | 6570 | 2.23 |
| $^{109}$Ag | | | 348 | 1.14 | 368 | 7.33 | 2930 | 0.82 |
| $^{110}$Pd/$^{110}$Cd | 147 | 0.78 | 3250 | 1.50 | 1340 | 4.55 | 2750 | 0.83 |
| $^{112}$Cd/$^{112}$Sn | 59.3 | 10.2 | 129 | 12.0 | 258 | 10.9 | 200 | 4.20 |
| $^{116}$Cd/$^{116}$Sn | 34.3 | 47.7 | 215 | 4.22 | 152 | 21.8 | 199 | 8.64 |
| $^{117}$Sn | | | 162 | 13.1 | | | 125 | 1.98 |
| $^{118}$Sn | | | 192 | 8.43 | | | 165 | 11.3 |
| $^{119}$Sn | | | 393 | 3.71 | 634 | 1.73 | 761 | 1.03 |
| $^{120}$Sn | | | 244 | 11.9 | 216 | 3.18 | 221 | 8.26 |
| $^{121}$Sb | 40.7 | 27.5 | 265 | 6.80 | 151 | 14.1 | 1720 | 4.02 |
| $^{122}$Sn/$^{122}$Te | | | 283 | 7.80 | 122 | 0.44 | 255 | 6.73 |
| $^{123}$Sb | | | 295 | 1.95 | | | 1420 | 0.52 |
| $^{124}$Sn/$^{124}$Te | | | 544 | 0.22 | | | 447 | 18.0 |
| $^{125}$Te/$^{125}$Sb | | | 357 | 7.71 | | | 319 | 12.6 |
| $^{126}$Sn/$^{126}$Te | | | 4040 | 1.03 | 1470 | 9.14 | 3410 | 3.06 |
| $^{128}$Te | | | 2840 | 0.84 | 768 | 6.50 | 2420 | 1.07 |
| $^{130}$Te/$^{130}$Ba | | | 10700 | 1.57 | 3060 | 1.46 | 9940 | 3.35 |
| $^{133}$Cs | 68.4 | 22.3 | 137 | 8.22 | 353 | 10.8 | 252 | 21.8 |
| $^{134}$Cs/$^{134}$Ba | | | 119 | 15.9 | | | 174 | 6.84 |
| $^{135}$Cs/$^{135}$Ba | | | 45.1 | 31.7 | | | 108 | 11.8 |
| $^{137}$Cs/$^{137}$Ba | | | 169 | 5.49 | 338 | 1.96 | 323 | 0.40 |
| $^{138}$Ba | 32.4 | 52.3 | 380 | 7.79 | 509 | 5.95 | 594 | 11.8 |
| $^{139}$La | | | 133 | 2.50 | 235 | 7.93 | 228 | 2.15 |
| $^{140}$Ce | | | 122 | 6.96 | 230 | 8.44 | 208 | 1.40 |
| $^{141}$Pr | 41.4 | 30.6 | 107 | 7.84 | 224 | 0.07 | 184 | 3.00 |
| $^{142}$Ce/$^{142}$Nd | | | 99.2 | 2.98 | 222 | 13.7 | 211 | 2.29 |
| $^{143}$Nd | | | 47.6 | 4.62 | | | 111 | 14.7 |
| $^{144}$Nd/$^{144}$Sm | | | 98.8 | 6.66 | 195 | 7.85 | 228 | 5.34 |
| $^{145}$Nd | | | 49.4 | 5.80 | | | 80.0 | 9.86 |
| $^{146}$Nd | | | 65.1 | 9.85 | | | 139 | 20.8 |

| Isotope(s) | Cell Blank (µg/g) | RSD (%) | NADS-1 Stage 1 (µg/g) | RSD (%) | NADS-1 Stage 3 (µg/g) | RSD (%) | NADS-2 Stage 3 (µg/g) | RSD (%) |
|---|---|---|---|---|---|---|---|---|
| $^{148}Nd/^{148}Sm$ | | | 37.1 | 6.38 | 102 | 14.4 | 92.4 | 14.4 |
| $^{150}Nd/^{150}Sm$ | | | 36.8 | 27.0 | | | 78.1 | 1.50 |
| $^{184}W$ | | | 34.1 | 19.5 | | | | |
| $^{191}Ir$ | | | 52.4 | 14.7 | 296 | 24.5 | 185 | 6.77 |
| $^{235}U$ | | | 143 | 13.1 | 233 | 0.67 | 299 | 10.0 |
| $^{236}U$ | | | 164 | 13.1 | 416 | 3.08 | 442 | 14.3 |
| $^{238}U$ | 49.9 | 35.1 | 28300 | 2.67 | 53900 | 3.43 | 62300 | 1.36 |
| $^{239}Pu$ | | | 2920 | 4.43 | 1310 | 0.69 | 2770 | 3.41 |
| $^{240}Pu$ | | | 1570 | 3.91 | 554 | 20.3 | 1660 | 1.23 |
| $^{241}Am/^{241}Pu$ | | | 666 | 11.8 | 251 | 6.20 | 687 | 0.02 |
| $^{242}Pu$ | | | 720 | 4.76 | 238 | 35.0 | 749 | 14.3 |
| $^{243}Am$ | | | 50.9 | 12.1 | | | 52.9 | 13.6 |
| $^{244}Cm$ | | | | | | | 98.8 | 40.9 |

TABLE 10
Elemental concentration from ICP-AES analysis

| Element | Cell Blank (µg/g) | RSD (%) | NADS-1 Stage 1 (µg/g) | RSD (%) | NADS-1 Stage 3 (µg/g) | RSD (%) | NADS-2 Stage 3 (µg/g) | RSD (%) |
|---|---|---|---|---|---|---|---|---|
| Ag | 581 | 11 | 829 | 15 | 2169 | 15 | 3609 | 15 |
| Al | 1360 | 19 | 6670 | 21 | 6660 | 21 | 8510 | 21 |
| B | < 176 | MDA | < 143 | MDA | < 690 | MDA | < 349 | MDA |
| Ba | < 118 | MDA | 777 | 10 | 1010 | 13 | 1340 | 10 |
| Be | < 11 | MDA | < 8.91 | MDA | < 43.1 | MDA | < 21.8 | MDA |
| Ca | 2140 | 10 | 40 | 14 | 6330 | 14 | 2090 | 14 |
| Cd | < 35 | MDA | < 28.3 | MDA | < 137 | MDA | < 69.3 | MDA |
| Ce | < 660 | MDA | < 534 | MDA | < 2590 | MDA | < 1310 | MDA |
| Co | < 85 | MDA | < 68.8 | MDA | < 333 | MDA | < 168 | MDA |
| Cr | < 139 | MDA | 1370 | 10 | 755 | 35 | 1030 | 12 |
| Cu | < 273 | MDA | < 266 | MDA | < 1070 | MDA | < 541 | MDA |
| Fe | 278 | 13 | 13222 | 16 | 7342 | 16 | 6272 | 16 |
| Gd | < 136 | MDA | < 110 | MDA | < 533 | MDA | < 269 | MDA |
| K | < 2000 | MDA | < 1620 | MDA | < 7850 | MDA | < 3960 | MDA |
| La | < 100 | MDA | < 81 | MDA | < 392 | MDA | < 198 | MDA |
| Li | < 756 | MDA | < 612 | MDA | < 2960 | MDA | < 1500 | MDA |
| Mg | < 25 | MDA | 501 | 10 | 408 | 10 | 292 | 10 |
| Mn | < 20 | MDA | 211 | 10 | 431 | 15 | 133 | 36 |
| Mo | < 626 | MDA | 88500 | 10 | 25900 | 10 | 114000 | 10 |
| Ni | < 235 | MDA | 700 | 10 | < 922 | MDA | 507 | 15 |
| P | < 849 | MDA | < 687 | MDA | < 3330 | MDA | < 1680 | MDA |
| Pb | < 731 | MDA | < 592 | MDA | < 2870 | MDA | < 1450 | MDA |
| S | < 7500 | MDA | < 6070 | MDA | < 29400 | MDA | < 14900 | MDA |
| Sb | < 688 | MDA | 563 | 31 | < 2700 | MDA | 3180 | 16 |
| Si | < 231 | MDA | 7510 | 10 | 2630 | 10 | 4140 | 10 |
| Sn | < 429 | MDA | 2570 | 11 | < 1680 | MDA | 2140 | 15 |
| Sr | 19 | 10 | 47.4 | 14 | 175 | 14 | 157 | 14 |
| Th | < 891 | MDA | < 721 | MDA | < 3490 | MDA | < 1760 | MDA |
| Ti | < 74 | MDA | 162 | 11 | < 290 | MDA | 224 | 12 |
| U | < 8680 | MDA | 31100 | 11 | 66000 | 13 | 73500 | 11 |
| V | < 52 | MDA | < 42.1 | MDA | < 204 | MDA | < 103 | MDA |
| Zn | < 39 | MDA | 229 | 11 | 1090 | 10 | 262 | 10 |
| Zr | 83800 | 10 | 59200 | 14 | 256200 | 14 | 101200 | 14 |

MDA – minimum detection of analysis

TABLE 11
EDS results corresponding to the points specified in Figures 2-4

| EDS Point Analysis | O | Zr | Mo | Tc | Ru | Rh | Pd | Ag | Te | Cd | U | Pu |
|---|---|---|---|---|---|---|---|---|---|---|---|---|
| | | | | | | (atom %) | | | | | | |
| 1 (Figure 2) | 83.3 | 1.8 | 3.9 | 0.0 | 5.6 | 0.2 | 3.5 | 0.4 | - | 0.8 | 0.4 | 0.0 |
| 2 (Figure 2) | 73.1 | 7.0 | 10.5 | 0.0 | 3.6 | 0.3 | 2.5 | 0.3 | - | 1.4 | 1.2 | 0.1 |
| 3 (Figure 2) | 73.7 | 25.2 | 0.0 | 0.0 | 0.5 | 0.0 | 0.3 | 0.0 | - | 0.2 | 0.0 | 0.0 |
| 4 (Figure 2) | 78.8 | 2.3 | 4.7 | 0.2 | 6.9 | 0.4 | 4.7 | 0.6 | - | 1.1 | 0.4 | 0.0 |
| 5 (Figure 2) | 87.1 | 2.1 | 3.4 | 0.0 | 3.6 | 0.1 | 2.3 | 0.3 | - | 0.7 | 0.4 | 0.1 |
| 1 (Figure 3) | 83.4 | 1.8 | 3.4 | 0.2 | 4.8 | 0.3 | 2.8 | 0.3 | 1.0 | 0.3 | 1.7 | 0.2 |
| 2 (Figure 3) | 82.9 | 2.1 | 2.5 | 0.2 | 4.6 | 0.3 | 2.9 | 0.4 | 1.3 | 0.4 | 1.6 | 0.7 |
| 3 (Figure 3) | 77.7 | 1.9 | 5.5 | 0.4 | 8.3 | 0.1 | 4.7 | 0.1 | 0.4 | 0.7 | 0.2 | 0.0 |
| 4 (Figure 3) | 80.6 | 1.8 | 3.2 | 0.2 | 5.6 | 0.2 | 3.6 | 0.3 | 1.5 | 0.5 | 2.0 | 0.5 |
| 5 (Figure 3) | 84.2 | 2.8 | 2.9 | 0.3 | 4.5 | 0.0 | 2.6 | 0.2 | 0.7 | 0.3 | 0.9 | 0.4 |
| 6 (Figure 3) | 81.3 | 2.3 | 4.9 | 0.2 | 6.4 | 0.0 | 3.9 | 0.2 | 0.2 | 0.6 | 0.2 | 0.0 |
| 1 (Figure 4) | 76.2 | 1.1 | 8.3 | 1.4 | 7.2 | 0.3 | 4.3 | 0.5 | 0.4 | 0.1 | 0.1 | 0.0 |
| 2 (Figure 4) | 78.8 | 4.1 | 4.9 | 0.6 | 7.0 | 0.0 | 3.5 | 0.4 | 0.5 | 0.1 | 0.1 | 0.0 |
| 3 (Figure 4) | 72.1 | 3.8 | 6.1 | 0.6 | 9.6 | 0.4 | 5.4 | 0.6 | 0.7 | 0.4 | 0.2 | 0.0 |
| 4 (Figure 4) | 72.2 | 26.4 | 0.6 | 0.0 | 0.3 | 0.0 | 0.2 | 0.0 | 0.1 | 0.0 | 0.1 | 0.0 |
| | | | | | | (mass %) | | | | | | |
| 1 (Figure 4) | 33.8 | 2.8 | 22.2 | 3.8 | 20.2 | 0.9 | 12.7 | 1.6 | 1.3 | 0.3 | 0.5 | 0.0 |
| 2 (Figure 4) | 37.2 | 11.0 | 13.9 | 1.7 | 20.8 | 0.1 | 11.1 | 1.3 | 1.5 | 0.4 | 1.0 | 0.0 |
| 3 (Figure 4) | 29.0 | 8.6 | 14.8 | 1.4 | 24.5 | 1.0 | 14.4 | 1.8 | 1.9 | 1.2 | 1.4 | 0.0 |
| 4 (Figure 4) | 31.1 | 64.7 | 1.6 | 0.0 | 0.9 | 0.0 | 0.6 | 0.0 | 0.4 | 0.1 | 0.5 | 0.1 |

TABLE 12
NADS-1, Stage-1, and Blank ICP-MS and ICP-AES estimated results

| | NADS-1, Stage-1 | | | | | | | | | | | |
|---|---|---|---|---|---|---|---|---|---|---|---|---|
| | Unknown | Zr | Mo | Tc | Ru | Rh | Pd | Ag | Cd | U | Nb | Other |
| | | | | | | (mass %) | | | | | | |
| ICP-MS | 47.9 | 13.3 | 8.0 | 0.8 | 12.9 | 4.1 | 6.7 | 0.7 | 1.7 | 2.9 | 0.3 | 0.9 |
| ICP-AES | 68.6 | 14.3 | 8.9 | - | - | - | - | - | - | 3.1 | - | 2.2 |

| | Blank | | | | | | | | | | | |
|---|---|---|---|---|---|---|---|---|---|---|---|---|
| | Unknown | Zr | Mo | Tc | Ru | Rh | Pd | Ag | Cd | U | Nb | Other |
| | | | | | | (mass %) | | | | | | |
| ICP-MS | 91.1 | 7.9 | - | - | - | - | - | - | - | - | - | 0.9 |
| ICP-AES | 88.6 | 8.4 | - | - | - | - | - | - | - | - | - | 3 |

TABLE 13
Epsilon particle chemical composition [8]

| Element | Composition (mass %) |
|---|---|
| Mo | 32.7 |
| Ru | 40.5 |
| Tc | 7 |
| Rh | 4.4 |
| Pd | 12.2 |
| Te | 3.8 |

TABLE 14
Mass Ratios of epsilon element concentrations from reference [8] and EDS point analyses 1, 2, and 3 from Figure 4

| Ratio | Ref. [8] | EDS Point 1 | EDS Point 2 | EDS Point 3 |
|---|---|---|---|---|
| Mo/Ru | 0.8 | 1.1 | 0.7 | 0.6 |
| Mo/Tc | 4.7 | 5.9 | 8.4 | 10.3 |
| Mo/Rh | 7.4 | 23.6 | 116.3 | 14.6 |
| Mo/Pd | 2.7 | 1.8 | 1.3 | 1.0 |
| Mo/Te | 8.6 | 67.2 | 31.0 | 11.9 |

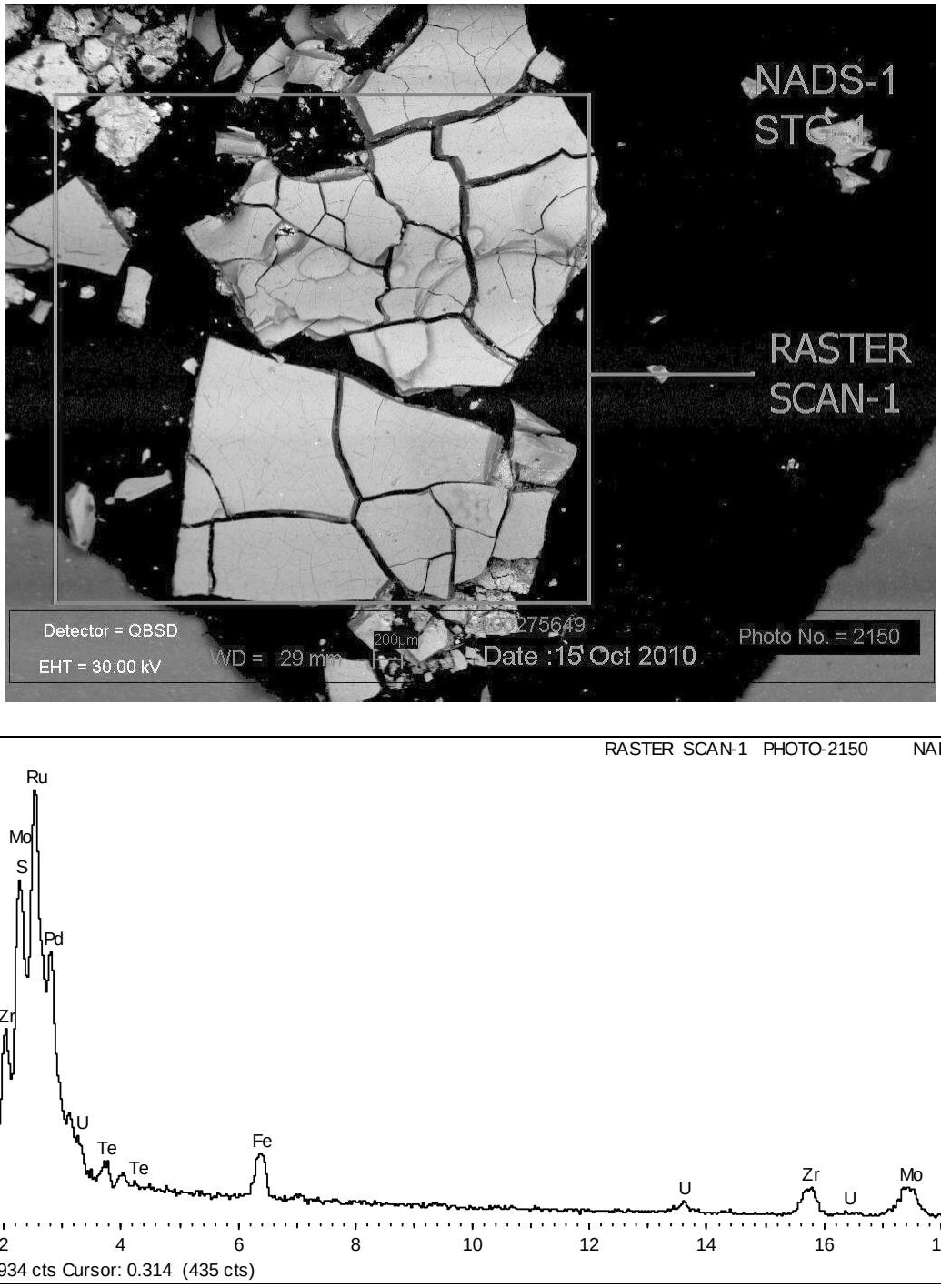


FIG. 1. Photomicrograph and raster scan for UDS sample NADS-1, Stage 1

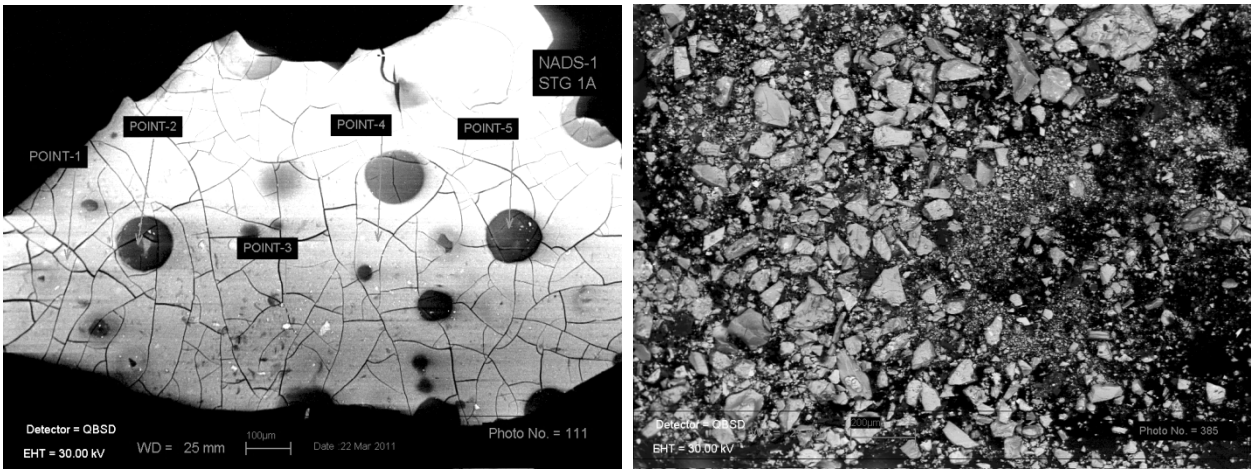


(a) (b)

FIG. 2. Uncrushed (a) and crushed (b) UDS samples from NADS-1, Stage-1. The uncrushed UDS sample had characteristics of a 'filter cake' conglomeration.

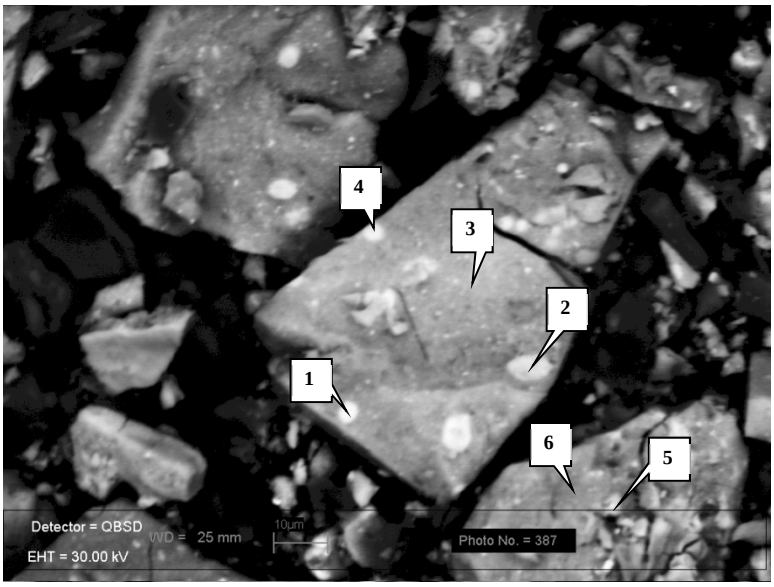


FIG. 3. Crushed surface of a UDS sample

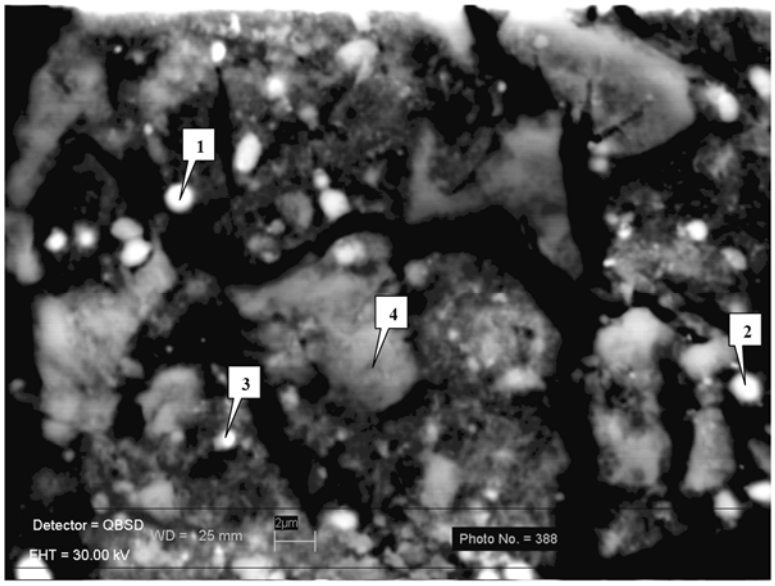

FIG. 4. High magnification of a crushed UDS sample

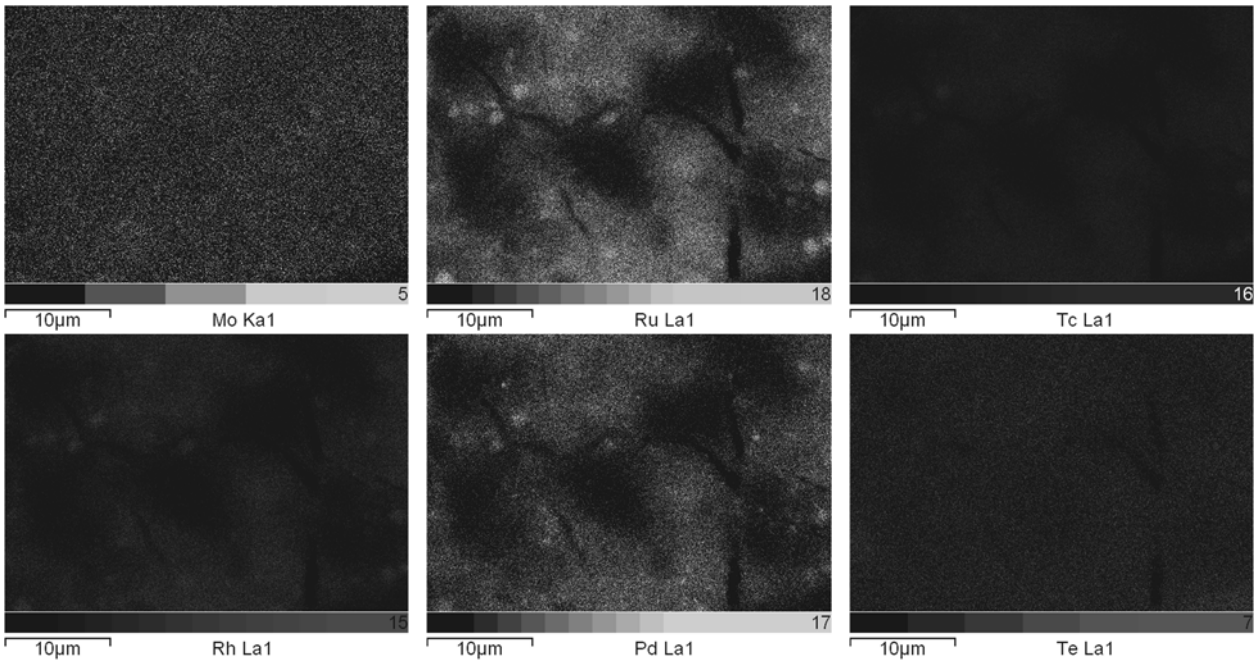

FIG. 5. EDS x-ray maps of possible epsilon particles in UDS. The image was converted to greyscale from color, and contrast and brightness were adjusted to attempt to retain useful concentration differentiation information.